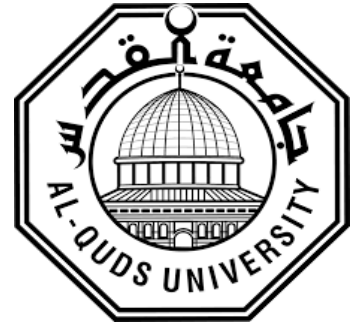


**Deanship of Graduate Studies  
Al-Quds University**



**The Efficiency of FLAIR-Weighted Blade in Motion  
Artifact Correction in Axial Brain MRI**

Prepared By: Maram Mohammad Mote Ghazawnah

M.Sc. Thesis

Jerusalem- Palestine

1444/2023

The Efficiency of FLAIR-Weighted Blade in Motion  
Artifact Correction in Axial Brain MRI

Prepared By: Maram Mohammad Mote Ghazawnah

B.Sc. of Medical Imaging, Al-Quds University / Palestine

Supervisor: Dr.Mohammad Hjoui

A Thesis Submitted in Partial Fulfilment of Requirements  
for the Degree Master of Medical Imaging Technology/  
Functional Imaging Track/ Faculty of Health Professions/  
Al-Quds University

Jerusalem- Palestine

1444/2023

Al-Quds University  
Deanship of Graduate Studies  
Faculty of Health profession  
Medical Imaging Technology



## Thesis Approval

### The Efficiency of FLAIR-Weighted Blade in Motion Artifact Correction in Axial Brain MRI

Prepared By: Maram Mohammad Mote Ghazawnah

Registration Number: 22011834

Supervisor: Dr. Mohammad Hjoui

**Master Thesis submitted and accepted, Date: 13.03.2023**

The name and signatures of the examining committee members are as follows:

1- Head of the committee: Dr. Mohammad Hjoui

Signature:

2- Internal Examiner: Dr. Sawsan Abu Sharkh

Signature:

3- External Examiner: Dr. Ali Abu Arra

Signature:

Jerusalem-Palestine

1444 / 2023

# **Dedication**

This Research is Dedicated to

My Dear Parents, Family, Instructors, and Colleagues

## **Declaration**

I certify that this thesis submitted for the degree of master, is the result of my own research, except where otherwise acknowledged, and that thesis has not been submitted for a higher degree to any other university or institution.

Signed  Maram

Maram Mohammad Mote Ghazawnah

Date:20/03/2023

## **ACKNOWLEDGEMENT**

I pray that Allah will grant us all the blessings that he has for us. I would also like to extend my gratitude to Dr. Mohammad Hjoug for sponsoring my studies and to ALLMED center for their help and support. Finally, I want to thank my husband for his assistance and encouragement.

Maram Mohammad Mote Ghazawneh

## Abstract

Magnetic resonance imaging (MRI) is a medical tool that can provide detailed information about the inner structure of a person's body. The use of the fluid-attenuated inversion recovery (FLAIR) sequence in imaging the brain is very useful, as it can help identify subtle changes in the brain's structure and function. Due to the sensitivity of MRI to artifacts, it is not always possible to achieve high-quality imaging. The presence of motion artifacts can affect the overall diagnostic value. In this study dipole filling for k-space (BLADE) was implemented for 46 different images with different motion types including right rotation, left rotation, right bending, left bending, flexion, extension, and combination. In this work, we aimed to measure signal-to-noise ratio (SNR), contrast-to-noise ratio (CNR), and percentage of signal ghosting (PSG). RADIANT DICOM viewer was used to calculate signal intensity (SI) and its standard deviation (SD), the SD is used as the noise index. ImageQC was used to calculate PSG while these measurements are plotted in Microsoft Excel. In this research, we used a control group of 46 patients who have standard images which use the cartesian filling for k-space for comparing the measurements with standard FLAIR sequence. Results showed using BLADE lead to a significant improvement in SNR, CNR, and ghosting in almost all types of motion while failing to correct ghosting from severe patient motion. The mean value of SNR was 1.08 for the dipole filling (BLADE) sequence and significantly reduced to 0.92 for the routine sequence ( $p < 0.05$ ). While the mean CNR was 0.75 for dipole filling and significantly reduced to 0.49 for routine sequence ( $p < 0.05$ ). Finally, the mean PSG for dipole filling was 0.75 and significantly reduced to 0.18 for routine sequence ( $p < 0.05$ ). In conclusion, the dipole filling sequence enhances SNR, and CNR due to flow and eye motion. Although BLADE reduced ghosting artifacts in most types of motion, BLADE was unable to eliminate ghosting appearance from the severe patient motion.

## Table of Contents

	<b>Page</b>
Declaration.....	i
ACKNOWLEDGEMENT.....	ii
Abstract.....	iii
Table of Contents.....	iiv
List of Figures.....	vi
List of Tables.....	viii
List of Abbreviations.....	ix
Chapter 1: Introduction.....	1
1.1 Background of the Study.....	1
1.2 Problem Statement.....	3
1.3 Justifications.....	4
1.4 Study Objective.....	4
Chapter 2: Literature Review.....	5
2.1 Motion Artifact.....	5
2.1.1 Types of Motion.....	6
2.1.2 Artifact Mitigation Strategiesn.....	7
2.2 Previous Studies.....	7
Chapter 3: Materials and Methods.....	10
3.1 MRI Imaging Acquisition.....	10
3.2 Data Analysis.....	11
3.2.1 Quantification of Motion.....	11
3.2.2 Image Quality.....	12
3.2.3 Statistical Analysis.....	15



Chapter 4: Results and discussion .....	16
4.1 SNR Values .....	16
4.2 CNR Values .....	18
4.3 PSG.....	21
Chapter 5: Conclusion and Recommendation .....	26
5.1. Conclusion.....	26
5.2. Recommendation.....	26
References .....	27
الملخص.....	31

## List of Figures

	Page
<b>Figure 1:</b> (A) Cartesian filling for k-space. (B) dipole filling for k-space (BLADE).	24
<b>Figure 2:</b> Radiant Dicom viewer logo (A). FLAIR axial image with 3 regions of interest (ROIs) drawn inside it (B).	26
<b>Figure 3:</b> Image QC v2.05 logo (A). Axial FLAIR image with the approach used to measure the percentage of signal ghosting PSG (B).	26
<b>Figure 3:</b> The percentage of signal ghosting (PSG) measurements approach, where the box size is 200mm X 20mm to measure the whole ghosting around the slice.	27
<b>Figure 5:</b> Signal noise ratio (SNR) for BLADE and cartesian (standard) sequence, the trend line of blade sequence SNR higher than standard sequence trend line due to repeated acquisition.	30
<b>Figure 6:</b> The left side shows the cartesian filling of k-space while the right side shows the dipole filling. The gray pixel shows normal sampling, while the black pixel shows oversampling.	31
<b>Figure 7:</b> The contrast to noise ratio (CNR) between cerebrospinal fluid (CSF) and fat, the trend line of CNR of the BLADE sequence is higher than the CNR trend line of the standard sequence due to increased SNR and noise reduction.	32
<b>Figure 8:</b> The contrast to noise ratio (CNR) between cerebrospinal fluid (CSF) and fat, the trend line of CNR of the BLADE sequence is higher than the CNR trend line of the standard sequence due to increased SNR and noise reduction.	33
<b>Figure 9:</b> Axial liver MRI with fat suppression image adapted from a study by Sumire Nanko et al. in 2009, shows the same finding obtained in figure 7. Fat suppression is more efficient in the Cartesian image as shown in (the left-hand side image).	33
<b>Figure 10:</b> Percentage of signal ghosting (PSG) for BLADE and standard sequence. BLADE curve oscillates in the range between (0% and 1.91%) while the standard sequence PSG is less than 0.5% for all patients, the data exhibit ascending	34

arrangement, and the PSG trend line of the BLADE sequence is higher than the PSG of the cartesian sequence both trend lines exhibit positive slope the PSG increase in BLADE sequence due to an increase of motion in phase encoding direction.

**Figure 11:** Left side image: arrow represent flow motion effect. Right side image: arrow represent eye movement effects on the image that appeared as a ghost artifact. **35**

**Figure 4:** Ghost artifacts on the left side and inside of the image. **36**

**Figure 5:** In-plan motion of the patient's head. The red line represents the slice section and patient motion in the range of the slice, so there was no data from outside the selected slice. **37**

**Figure 6:** Cross-plan motion for the head. The slice section had changed and data were obtained from outside the slice. **37**

## List of Tables

	<b>Page</b>
<b>Table 1:</b> MRI parameter for standard FLAIR and BLAD protocol.	<b>23</b>
<b>Table 2:</b> MRI Image number and motion protocol where number 1 in the motion protocol column means flexion, 2: Extension, 3: Left rotation, 4: Right rotation, 5: Left bending, and 6: Right bending.	<b>25</b>

## List of Abbreviation

---

<b>2D</b>	Tow dimensional
<b>3D</b>	Three dimensional
<b>AVM</b>	Arteriovenous malformation
<b>BLADE</b>	Motion Correction with Radial Blades
<b>BW</b>	Bandwidth
<b>COVID-19</b>	Coronavirus disease
<b>DICOM</b>	Digital Imaging and Communications in Medicine
<b>DWI</b>	Diffusion-weighted imaging
<b>ETL</b>	Echo train length
<b>FLAIR</b>	Fluid-attenuated inversion recovery
<b>FOV</b>	Field of view
<b>FSE</b>	Fast spin-echo
<b>GE</b>	General Electric
<b>GRAPPA</b>	GeneRalized Autocalibrating Partial Parallel Acquisition
<b>HASTE</b>	Half-Fourier-Acquired Single-shot Turbo spin Echo
<b>mm</b>	Millimeter
<b>MR</b>	Magnetic resonance
<b>MRI</b>	Magnetic resonance imaging
<b>NEX</b>	Number of excitations
<b>PAT</b>	Parallel acquisition techniques
<b>PE</b>	Phase encoding
<b>PROPELLER</b>	Periodically rotated overlapping parallel lines with enhanced reconstruction
<b>PSG</b>	Percentage of signal ghosting

---

<b>ROI</b>	Region of interest
<b>SI</b>	Signal intensity
<b>SI<sub>A</sub></b>	Signal intensity of A
<b>SNR</b>	Signal-to-noise ratio
<b>T</b>	Tesla
<b>TE</b>	Echo time
<b>TR</b>	Repetition time
<b>TSE</b>	Standard turbo spin-echo

---

# Chapter 1

## Introduction

### 1.1 Background of the Study

Magnetic Resonance Imaging (MRI) is a medical tool that can provide detailed information about the inner structure of a person's body. It can also visualize various types of soft tissues, such as the brain, spinal cord, and abdominal organs. Through its wide variety of techniques, MR allows us to distinguish between different types of tissues. MRI scan has many advantages of MRI for the diagnosis of soft tissue issues. However, there are many challenges that it can face in the clinical and research arenas. One of these is the time-consuming data acquisition process which increases the motion-related challenges. Other factors such as the complexity of the procedure, problems with the presence of metal implants, and the need for specialized expertise can also affect the use of MRI (Andre et al. 2015).

Different types of MRI sequences are used during a routine imaging procedure. The fluid-attenuated inversion recovery (FLAIR) sequence is a special type that can remove the signal from the spinal fluid. On the images, brain tissue on the FLAIR sequence appears similar to those of T2 weighted images but the cerebral spinal fluid (CSF) has a dark signal. The use of the FLAIR sequence in imaging the brain is very useful, as it can help identify subtle changes in the brain's structure and function. This is especially true in the detection of changes in the periventricular region and the periphery of the hemisphere. The usefulness of this sequence has been evaluated in various neurological disorders, such as multiple sclerosis and infarction (Siegelman ES n.d.).

Due to the sensitivity of MRI to artifacts, it is not always possible to achieve high-quality imaging. In addition to reducing the relevance of the data, this issue can also affect image quality. Some of the common motion artifacts that can occur during the acquisition process include ghosting, blurred, and geometric distortion which will reduce the overall signal-to-noise ratio (SNR) and diagnostic value. The presence of motion artifacts can affect the efficiency of a technologist's work. It can also lead to repeat acquisition

sequences, which can prolong the examination time and affect the patient's comfort. The relevance of artifacts such as those found in medical images depends on the reader's ability to identify and separate them from the structures of interest and the pathologies they mimic. In the case of non-diagnostic data degradation, repeated scans or the entire session could lead to a delay in treatment and higher costs (Lin Zhang, ChunMei Tian, PeiYuan Wang, Liang Chen, XiJin Mao, ShanShan Wang, Xu Wang 2015).

Various methods can be used to correct the motion, and they can be categorized according to their requirements. For instance, the motion can be rigid or non-rigid. It can occur between the volumes of an image or between the signals acquired and the excitations. The amount of motion that can be observed during an acquisition period is relevant to the spatial resolution of the object. There are various types of motion patterns that can be used to describe this process, such as continuous, quasi-periodic, or random. In two dimensional and 3D imaging, the motion within a slice plane is referred to as in-plane motion, while the motion to the slice is referred to as through-plane motion. In contrast, in three-dimensional 3D imaging, the difference between two motions is not required (Boussel et al. 2006).

Manufacturers of MRI equipment have developed imaging sequences that can reduce artifacts. For instance, standard turbo spin-echo (TSE) sequences are used to fill the k-space during the repetition time (TR). They are acquired once or according to a set of multiple averages. However, the data collected in the center of the k-space has a significant impact on the quality of the images. The main technique used to reduce artifacts is by increasing the acquisition speed. This can be done through the use of various techniques such as the Half-Fourier-Acquired Echo (Huyen Thanh Nguyen, Zariné Ketul Shah, Amir Mortazavi, Kamal S Pohar, Lai Wei, Debra Lyn Zynger n.d.).

BLADE refers to a sequence of procedures that utilize the PROPELLER (periodically rotated overlapping parallel lines with enhanced reconstruction) method, which is a combination of rotating parallel lines and enhanced reconstruction introduced by SIEMENS Healthcare. In this method, several blades are used to generate a k-space trajectory. Each blade has its own lowest phase-encoding line, which is used to acquire the echo train length (Pipe 1999; Sedat Alibek, Boris Adamietz, Alexander Cavallaro, Alto



Stemmer, Katharina Anders, Manuel Kramer, Werner Bautz 2008). The turbo spin Echo sequence known as the BLADE is composed of multiple shots, each with its own motion-insensitive feature. Inter-shot motion correction, which is performed during each shot, is then used to reduce in-plane motion artifacts. Data is collected in parallel with phase-encoding lines. Each of the blades is rotated to cover a circle inside the raw data space (Yuusuke Hirokawa MD, Hiroyoshi Isoda PhD, Yoji S. Maetani PhD, Shigeki Arizono MD, Kotaro Shimada MD 2008). The use of the BLADE sequences has been widely marketed and is used in neuroradiologic and abdominal imaging procedures. They were initially used to reduce motion artifacts and improve the detection of lesions in diffusion-weighted imaging (DWI) (Lin Zhang, ChunMei Tian, PeiYuan Wang, Liang Chen, XiJin Mao, ShanShan Wang, Xu Wang 2015). In addition to reducing the motion artifacts in patients, BLADE can also help decrease the possibility of anesthesia in children and adults who are not cooperative (Pipe 1999; Sedat Alibek, Boris Adamietz, Alexander Cavallaro, Alto Stemmer, Katharina Anders, Manuel Kramer, Werner Bautz 2008).

The goal of motion artifact correction in brain MRI is to prevent or minimize the effects of motion on the functioning of the brain. Other fields that are involved in this process include liver, cardiac, and thorax MRI. However, due to the nature of the chest and heart's periodic movement, the approach to head motion correction has limited overlap. This study aims to analyze the effects of the FLAIR-BLADE sequence on the motion artifacts in the brain.

## **1.2 Problem Statement**

Motion artifacts are an inherent problem in magnetic resonance imaging (MRI). MRI has always been particularly sensitive to subject motion. This is primarily due to the prolonged time required for most MR imaging sequences to collect sufficient data to form an image. The appearance of motion artifacts in an image is a result of a complicated interaction between the image structure, the type of motion, the specifics of the MR pulse sequence and the k-space acquisition strategy. Movement artifacts in MRI degrade image quality and may lead to misinterpretation in the final diagnosis. In MRI sequences with robust visual interpretation, simple motion artifacts can be identified as ghosting or

blurring (Satterthwaite et al. 2012). While sensitivity to particle motion or blood flow can be used to provide useful image contrast, bulk motion presents a considerable problem in the majority of clinical applications. It is one of the most frequent sources of artifacts. Over 30 years of research have produced numerous methods to mitigate or correct motion artifacts, but no single method can be applied in all imaging situations (van Dijk, Sabuncu, and Buckner 2012).

### **1.3 Justifications**

Due to the presence of patient motion, it is estimated that up to 42% of MRI sequences may exhibit degradation. One of the most common methods of reducing imaging time is by implementing fast imaging techniques. This has led to a reduction in the time it takes to acquire images from several minutes to a few seconds. However, this method can also compromise the quality of the images (Andre et al. 2015). Several techniques have been proposed to solve the motion-correction problem. Although these techniques can sometimes be successful, they are not always effective. The development of new motion correction techniques has led to the improvement of image quality. With the use of the BLADE sequence, it can be used to reduce the motion artifact in the final image (Yuusuke Hirokawa MD, Hiroyoshi Isoda PhD, Yoji S. Maetani PhD, Shigeki Arizono MD, Kotaro Shimada MD 2008). The complexity of patient motion is a major challenge that affects the global MR community. This issue can lead to inefficient utilization of hospital resources, suboptimal interpretations, and throughput delays.

### **1.4 Study Objective**

1. To analyze the efficiency of the BLADE in the correction of (mild, moderate, and severe) motion artifacts during axial FLAIR-W brain MRI.
2. To evaluate the ability of BLADE in improving image quality criteria in terms of SNR, CNR, and ghosting.

## **Chapter 2**

### **Theory and Literature Review**

#### **2.1 Motion Artifact**

Due to the low sensitivity and signal loss associated with motion artifacts in MRI technology, the development of faster sequences has been hindered by this issue. This is why the introduction of more sophisticated equipment such as multichannel phased array coils has been instrumental in the advancement of this technology and using of gradient echo instead of the traditional spine or turbo spin echo (Andre et al. 2015).

MRI is known to be sensitive to the motion of the subjects. This is due to how long it takes for most sequences of MR imaging to collect enough data to produce an image. Motion has been known to have effects on the image since the very beginning of MRI. This includes ghosting and blurring in the data. It is longer than other types of physiological motion, such as involuntary movements. Vessel pulsation, blood flow, and cardiac and respiratory movements are examples of this (Andre et al. 2015; Siegelman ES n.d.). Advances in hardware have allowed faster imaging, and these include breakthroughs in parallel imaging and higher performance gradients. This is beneficial for moving spins as the stronger gradients mean that the phase accumulation will increase by utilizing a stronger gradient. With faster scans, there is a reduced chance of involuntarily moving subject matter. Furthermore, The stronger main field strengths and gradients of MRI scans can make them louder, which can reduce the chance that an infant will fall asleep during the procedure. This is especially true with diffusion-weighted imaging (Lin Zhang, ChunMei Tian, PeiYuan Wang, Liang Chen, XiJin Mao, ShanShan Wang, Xu Wang 2015).

There is currently no apparent solution to the subject motion issue in MRI examinations. The limitations of the current generation of imaging systems are mainly due to biological constraints. These include the use of a specific absorption rate (SAR), the restriction of switching gradient speeds, and the constraints on the repetition (TR) and echo times (TE). It is widely believed that there is not a single methodological solution for the design and implementation of motion correction in MRI. Instead, there are a variety of tools that can be utilized to address this issue.

The type of motion involved and the situation at hand dictate the choice of the appropriate tool. Some techniques, such as correction or prevention, are highly effective in certain situations, but they are useless in others. Understanding the various types of motion artifacts and their properties will allow you to identify the cause of the problem and use the best possible tool (Lin Zhang, ChunMei Tian, PeiYuan Wang, Liang Chen, XiJin Mao, ShanShan Wang, Xu Wang 2015).

### **2.1.1 Types of motion**

The different types of motion that are relevant to MRI can be loosely categorized into three categories: flow, elastic, and rigid body motion. For instance, rigid body motion can be described as a multi-dimensional translation of one parameter into another. It can also be completely unconstrained or require a single parameter to be represented. Although a one-dimensional translation can be used to describe the diaphragm motion, involuntary head movements usually require six degrees of freedom, which consists of three rotations and three translations. Besides being able to move rigidly, elastic motion can also include stretching, compression, and shear along three axes. It requires 12 degrees of freedom to fully represent its effects. In the abdomen, various deformations and displacements can be observed. For instance, it can be assumed that the flow in a small or medium-sized vessel is one-dimensional, while the flow in a CSF in the cervical spine is one-dimensional (Boussel et al. 2006).

This implies that the velocity required for its complete representation is only one parameter. The velocity vector field is required for the complete description of a given object. The most accurate approximation is the displacement field, which shows the trajectories of the particles within an object as a function of time. However, this field is not always accurate. For most practical applications, this description is too detailed. The various constraints that humans have on their bodies, such as the incompressibility of liquids and the presence of bones and joints, can drastically reduce the number of parameters that are needed to describe motion (Huyen Thanh Nguyen, Zarine Ketul Shah, Amir Mortazavi, Kamal S Pohar, Lai Wei, Debra Lyn Zynger n.d.).

### **2.1.2 Artifact Mitigation Strategies**

Many types of motion can affect data corruption, and various strategies can be used to address these issues. We will discuss the three main methods that are commonly used to address this issue: motion prevention, motion correction, and artifact reduction.

One of the most common ways to suppress motion artifacts is by preventing them from moving. This method can prevent the effects of the review from happening, but it is not always practical. This is why it is often necessary to use other methods such as motion correction or reduction. This review focuses on the concept of artifact reduction, which is a method that reduces the artifacts in an image by replacing them with less dramatic features. On the other hand, motion correction is a type of acquisition that involves the compensation and estimation of motion (Lin Zhang, ChunMei Tian, PeiYuan Wang, Liang Chen, XiJin Mao, ShanShan Wang, Xu Wang 2015).

### **2.2 Previous Studies**

A 3T MRI system with a double SNR provides advantages without increasing the scan time. However, it has drawbacks, such as the presence of pulsatile flow artifacts and susceptibility artifacts. With the use of a BLADE sequence, these can be eliminated. Recently, a new technique was developed to detect pulmonary damage caused by the coronavirus disease (COVID-19) (Alibek et al. 2008). In addition, the results of a study conducted at 3T revealed that the radial k-space data collected during the axial FLAIR BLADE procedure significantly improved the quality of images compared to the rectilinear sampling method (Wu, Zhang, and Zhang 2021).

In previous studies, the use of the PROPELLER/BLADE technique for the measurement of the k-space area in the cervical spine resulted in a significant increase in the number of artifacts in the axial orientation. In the cervical region, the presence of T2-BLADE in an axial orientation led to the blurring of the subarachnoid space. However, this area was not considered a significant feature in the evaluation of the spinal cord. Compared to TSE, axial BLADE was better in terms of spinal cord depiction (Wu et al. 2021).

In a previous study, the researchers compared the image quality and characterization of brain MR images of patients who were moving with the use of rectilinear and partially radial acquisition techniques. They found that the use of the FLAIR BLADE sequences significantly reduced the motion artifacts and pulsation artifacts (Mcrobbie et al. n.d.). Furthermore, In a previous study, they discovered that the use of the BLADE sequences in angiographies improved the visualization of the vessels. This led to the development of new techniques for performing angiographic procedures (Epistatou, Tsalafoutas, and Delibasis 2020). In a study conducted on renal MRI, Michaely et al (Henrik J. Michaely MD, Harald Kramer MD, Sabine Weckbach MD, Olaf Dietrich PhD, Maximilian F. Reiser MD 2008). found that the PROPELLER technique did not cause pulsation artifacts in the major vessels. They also noted that the higher number of disturbing artifacts in the standard TSE group was due to the sequence.

A study by Yuusuke Hirokawa et al. 2018 found that using the BLADE technique could improve the quality of the images by reducing the artifacts and increasing the k space coverage (Boussel et al. 2006). E. Lavdas et al. 2015 noted that the use of the BLADE sequences in shoulder imaging can help reduce pulsation and motion artifacts during the procedure. They also recommend it for patients who are not cooperative (Pipe 1999).

In 2011, Barton et al. evaluated the effects of the BLADE sequence on various aspects of imaging, such as the junctional zone, the depiction of follicles ( $p < 0.0001$ ), and the detection of female reproductive organs. They found that the sequence was superior to the conventional methods for these studies. In addition, the reduction in respiratory motion artifacts with the use of the BLADE sequence was also beneficial. However, the image quality was not affected by the presence of a radial artifact (Lin Zhang, ChunMei Tian, PeiYuan Wang, Liang Chen, XiJin Mao, ShanShan Wang, Xu Wang 2015).

Sedat Alibe et al. 2008, reported that the FLAIR BLADE imaging technique significantly reduced the motion artifacts and pulsation artifacts compared to the conventional spin-echo sequence scan. FLAIR BLADE images showed higher contrast-to-noise ratios and lower signal-to-noise ratios (Sedat Alibe 1 , Boris Adamietz, Alexander

Cavallaro, Alto Stemmer, Katharina Anders, Manuel Kramer, Werner Bautz 2008).

Another study conducted by Wintersperger et al. 2006 revealed that the PROPELLER acquisition technique minimizes motion artifacts and improves the image quality for brain MRI using a 3-Tesla scanner (Huyen Thanh Nguyen, Zarine Ketul Shah, Amir Mortazavi, Kamal S Pohar, Lai Wei , Debra Lyn Zynger n.d.).

## Chapter 3

### Materials and Methods

#### 3.1 MRI Imaging Acquisition

A 1.5T scanner (Magnetom ESSENZA; Siemens Medical System, Erlangen, Germany), Allmed medical center was used to perform a brain examination. Where the imaging parameters used to acquire images of each contrast with rectilinear and BLADE techniques, and the imaging parameters of those sequences are shown in Table 3.1. The sequences of the BLADE technique are almost identical to the conventional sequences in terms of their acquisition time and bandwidth. They also have larger echo training length (ETL) and bandwidth values with 100% BLADE coverage per line, which are important in reducing motion artifacts.

**Table 1:** MRI parameter for standard FLAIR and BLAD protocol.

Parameter	FLAIR	BLADE FLAIR
matrix	320 x 262	320 x 240
FOV	230 mm	230 mm
Slice Thickness	5 mm	5 mm
TR	5000 ms	4500 ms
TE	81 ms	148 ms
NEX	1	1
Concatenation	2	1
FOV Phase	93.8%	100%
BLADE Coverage	-	111.1%
BW	90	125
Turbo Factor	16	19
Trajectory	CARTESIAN	BLADE
PAT Mode	GRAPPA	OFF
Accel Factor	2	OFF
Reference Scan	Self-Calibration	Integral



Several MRI vendors, such as GE, Siemens, Philips, and Toshiba, offer their version of the motion correction technique known as k-space acquisition. This method is different from the conventional rectilinear method, as it involves collecting multiple blades in an overlapping radial style (Almuqbel et al. 2018). Figure 1 shows the standard cartesian filling for k-space and dipole filling for k-space of the BLADE.

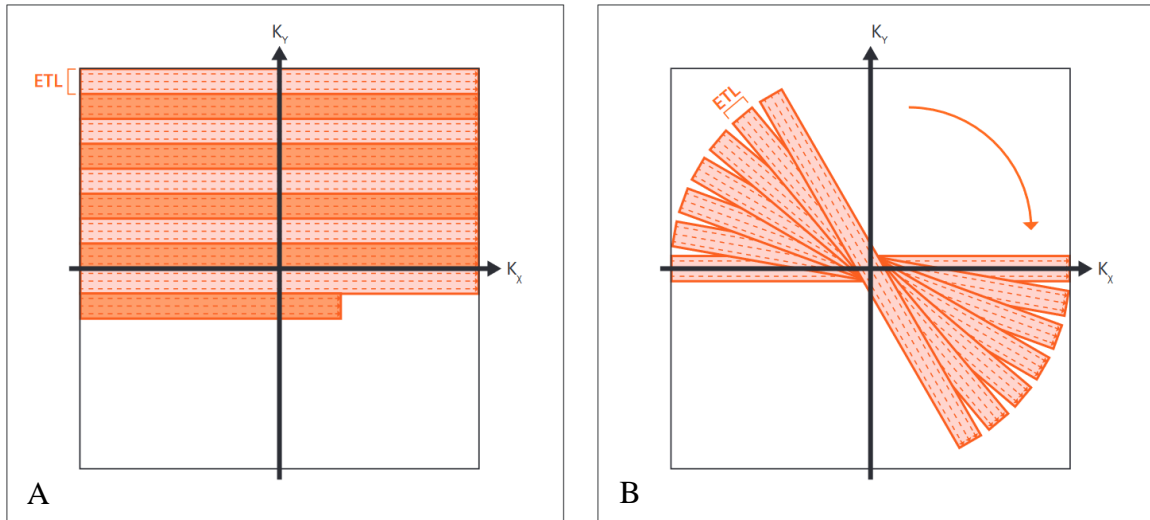


**Figure 7:** (A) Cartesian filling for k-space. (B) dipole filling for k-space (BLADE) (Wu et al. 2021).

## 3.2 Data Analysis

### 3.2.1 Quantification of Motion

The differences in head movement between a volunteer with different instruction conditions and a control group were measured. The FLAIR-weighted and the FLAIR BLADE images were used as references. Values of the 6 separate types of head movement (flexion, 2: extension, 3: left rotation, 4: right rotation, 5: left bending, 6: right bending) were included under each of the 6 instruction conditions (for a total of 46 slices) and listed in Table 3.2. Terms for all instruction of motions type were included in the model to allow for non-independence of the different slices from the same subject.

**Table 2:** MRI Image number and motion protocol where number 1 in the motion protocol column means flexion, 2: extension, 3: left rotation, 4: right rotation, 5: left bending, and 6: right bending.

MRI Image Number	Motion Protocol	MRI Image Number	Motion Protocol
1	standard	24	1+2+3
2	BLADE without motion	25	1+2+4
3	1	26	1+2+5
4	2	27	1+2+6
5	3	28	1+3+4
6	4	29	1+3+5
7	5	30	1+3+6
8	6	31	1+4+5
9	1+2	32	1+4+6
10	1+3	33	1+5+6
11	1+4	34	2+3+4
12	1+5	35	2+3+5
13	1+6	36	2+3+6
14	2+3	37	3+4+5
15	2+4	38	3+5+6
16	2+5	39	4+5+6
17	2+6	40	1+2+3+4
18	3+4	41	1+2+3+5
19	3+5	42	1+2+3+6
20	3+6	43	1+2+3+4+5
21	4+5	44	1+2+3+4+6
22	4+6	45	1+2+3+4+5+6 (once)
23	5+6	46	1+2+3+4+5+6(twice)

### 3.2.2 Image Quality

The image ghosting artifact was computed using the Image QC v2.05 software. RADIANT DICOM, which is a software used for analyzing images, also takes into account various image quality parameters such as contrast-to-noise ratios and signal-to-noise ratios. The quantitative analysis of the data included the following parameters: (a) the SNR of the whole image including the cerebral spinal fluid (CSF), white matter, grey matter, fat, rectus extraocular muscle, and background noise (b) the contrast-to-noise ratio (CNR) between fat and CSF (Figure 2.B) and (c) percentage of signal ghosting (PSG) (Figure 3.B).

Furthermore, the images will be compared with those of the patients who were acquired using the FLAIR protocol without any motion.

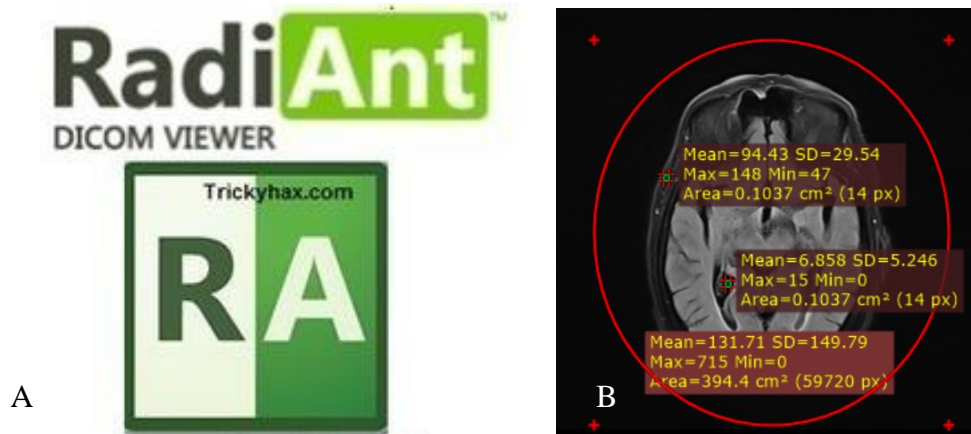


**Figure 8:** Radiant Dicom viewer logo (A). FLAIR axial image with 3 regions of interest (ROIs) drawn inside it (B).

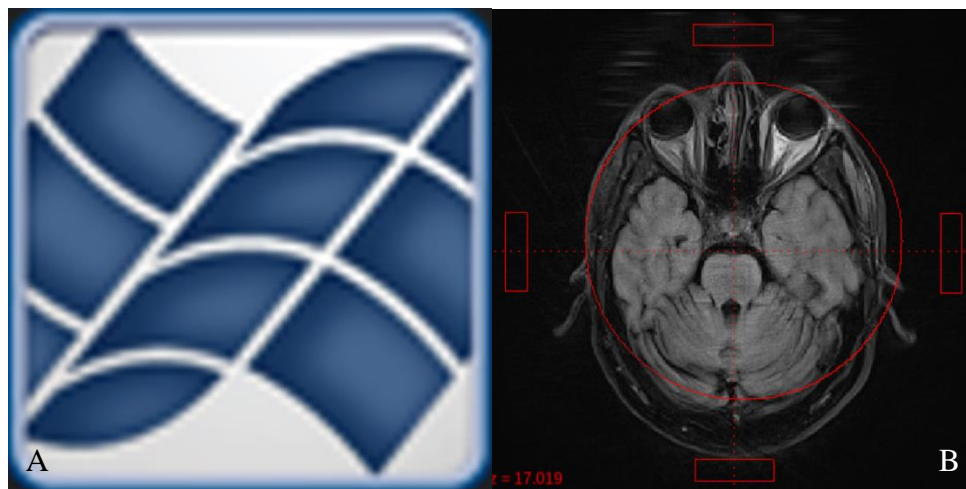


**Figure 9:** Image QC v2.05 logo (A). Axial FLAIR image with the approach used to measure the percentage of signal ghosting PSG (B).

For calculating the SNR, and CNR values, the signal intensity (SI) was measured with a large elliptical region of interest (ROI), which was placed at the whole image that included (CSF, white matter, grey matter, fat, rectus extraocular muscle, and background noise). The noise was defined as a standard deviation of the signal intensity. The size of the ROI used for SNR and noise was 369.5 cm<sup>2</sup>. This ROI for each patient was placed at an identical position and size on the comparison sequences. In some cases, the positions of the

ROI were adjusted due to patient movement. The SNR was calculated by the following mathematical equation (Mcrobbie et al. n.d.):

$$\text{SNR}_A = \text{SI}_A / N \dots\dots\dots(1)$$

where A represents the image or whole slice, the  $\text{SI}_A$  is the signal intensity of A measured by an (ROI), and N is the image noise, which was defined as the standard deviation (SD) of the SI.

The CNR was calculated based on the following formula (Mcrobbie et al. n.d.):

$$\text{CNR}_{AB} = (\text{SIA} - \text{SIB}) / N \dots\dots\dots(2)$$

where SIA and SIB define the SI of the tissues A (fat) and B (CSF), respectively.

The PSG was calculated based on the following formula (Epistatou et al. 2020):

$$\text{PSG} = 100 * ((\text{LET ROI} + \text{RIGHT ROI}) - (\text{TOP ROI} + \text{BOTTOM ROI})) / (2 * \text{center}) \dots\dots(3)$$

Where ROI size was adapted to cover the whole area outside the slice and the whole slice.

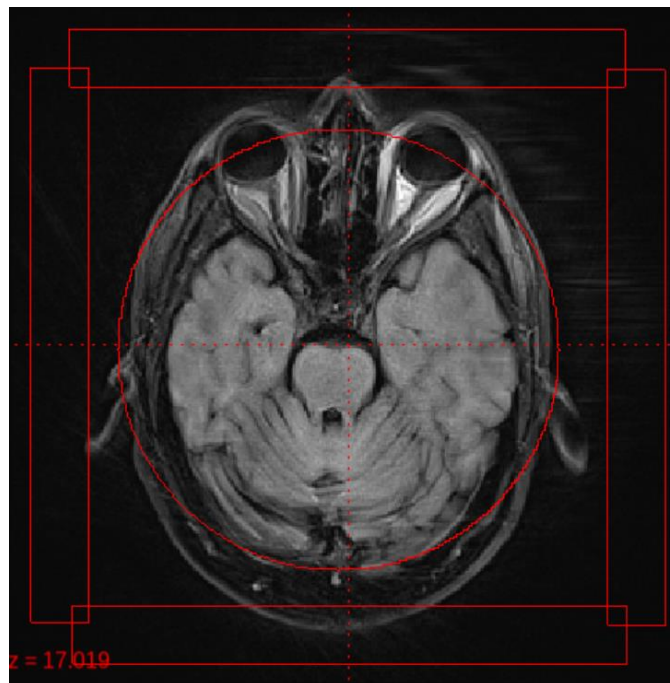


**Figure 4:** The percentage of signal ghosting (PSG) measurements approach, where the box size is 200mm X 20mm to measure the whole ghosting around the slice.

### **3.2.3 Statistical Analysis**

Inferential and descriptive statistical methods are used in the data manipulation process. The former focuses on the interpretation of the data while the latter is on the analysis of the data. This study was carried out using Microsoft Excel software. On the other hand, descriptive methods such as charts, percentages, and means were used by the study's to clarify the obtained results. The objective of the study was to compare the population means of two independent groups with the population standards of two unequal groups by using a statistical t-test. The  $p < 0.05$  was used significance standard.

## Chapter 4

### Results and discussion

#### 4.1 Signal to noise ratio (SNR)

The results of the quantitative analysis obtained from all the patients are presented in Figure 4.1 for the uncooperative and standard groups of patients. The minimum and maximum values of SNR for BLADE were (0.98 to 1.21) respectively. For the standard sequence, the minimum and maximum values of SNR were (0.76 to 1.1) respectively. For the uncooperative group of patients, the mean SNR values of the BLADE sequences is 1.08 which is slightly higher than the mean of those corresponding standard sequences that is 0.92. Furthermore, the differences between the BLADE and the corresponding standard sequences were found to be statistically significant in most of the cases examined  $p < 0.05$ .

In the BLADE sequences, SNR in CSF was lower compared with the standard FLAIR sequences. Similarly, in the standard group of patients, the FLAIR sequences had higher values than the corresponding BLADE sequences in the majority of the cases regarding the SNR measurements. In contrast to the conventional sequences, the pulsatile flow artefact's in the BLADE sequences were lower. In patients with an uncooperative condition, the standard deviation was also lower.

The results of the study presented by (Yuusuke Hirokawa et al, 2008) showed that the application of a dipole filling technique for k-space leads to an increase in its SNR. Due to repeated acquisition as shown in figure (1). Also, MRI protocol can be modified and the SNR affected by multiple factors.

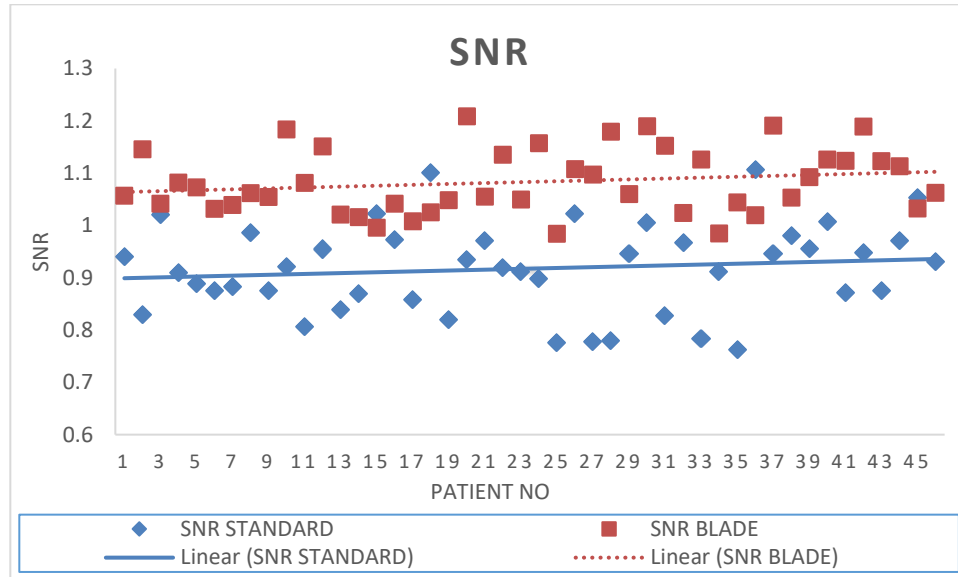


**Figure 5:** Signal noise ratio (SNR) for BLADE and cartesian (standard) sequence, the trend line of blade sequence SNR higher than standard sequence trend line due to repeated acquisition.

The use of a dipole filling technique for K-space (BLADE) can negatively affect the SNR if the partial acquisition technique (PAT) is used which improves the resolution and prevents blurring (Barton F. Lane<sup>1</sup>, Fauzia Q. Vandermeer<sup>1</sup>, Rasim C. Oz<sup>1 2</sup>, Eric W. Irwin<sup>1 3</sup> 2011). However, the results of this study show that the BLADE sequence effect is different and the SNR increased due to repeated acquisition and the use of complete filing of k-space instead of PAT.

In the obtained images during this work image, the difference between the standard sequence and the BLADE image was due to various factors, such as the use of BW in a narrower than standard dimension. This method can solve the issue of SNR reduction by modifying the MRI protocol (Shokrollahi, Drake, and Goldenberg 2017). Patients' age plays a role in the variation in their SNR. For instance, the younger patient has a higher SNR than the older patient, while the latter has a lower SNR (R. George, J. , Dela Cruz 2022). BLADE images were obtained from a young patient aged 31 years, while the standard sequence was obtained for different patients ages in the range between 18 and 82. Also, due to the increase in motion ghosting artifacts, the standard sequence is used for patients of varying ages. Finally, due to motion ghosting artifact increase and add a new pseudo signal that increases the SNR.

A study conducted by R. George et al, 2022 (R. George, J. , Dela Cruz 2022) shows that the obtained SNR for the BLADE sequence is higher than for the samples taken from a standard MRI protocol. The most important role in MRI protocol is lesion detectability, a study conducted by Yoshimitsu Ohgiya et all. 2010 revealed that the efficiency of the BLADE sequence in detecting lesions is similar to that of the cartesian sequence (Ohgiya et al. 2010). Furthermore, a study conducted by Eleftherios Lavdas et all. 2013 about lesion detection showed that the BLADE efficiency in detecting various types of lesions, such as AVM, orbits, and periventricular lesions, is similar to that of the cartesian sequence (Lavdas et al. 2013). References from 17-19 are not mentioned in the literature review

In our work, the increase in the SNR from the filling of k-space was due to the radial BLADE coverage adjustment to 100%, which resulted in the acquisition of the same k-space as follows (Figure 5). The contrast between the gray and black pixels shows that the center of the image is oversampled, while the periphery is normal and sometimes under-sampled (Tamhane and Arfanakis 2009).

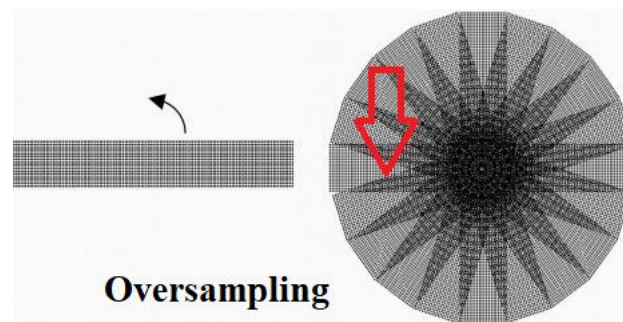


**Figure 6:** The left side shows the cartesian filling of k-space while the right side shows the dipole filling. The gray pixel shows normal sampling, while the black pixel shows oversampling.

#### **4.2 Contrast to noise ratio Values**

The minimum and maximum values of CNR for BLADE were (0.43 to 1.24) respectively. For the standard sequence the minimum and maximum values of CNR were (.013 to 0.94) respectively. In the uncooperative group of patients, the mean CNR values of the BLADE sequences is 0.75 which is slightly higher than the mean of those



corresponding standard sequences which is about 0.49. Furthermore, Figure 6 shows the differences between the BLADE and the standard sequences were found to be statistically significant in most of the cases examined  $p < 0.05$ .

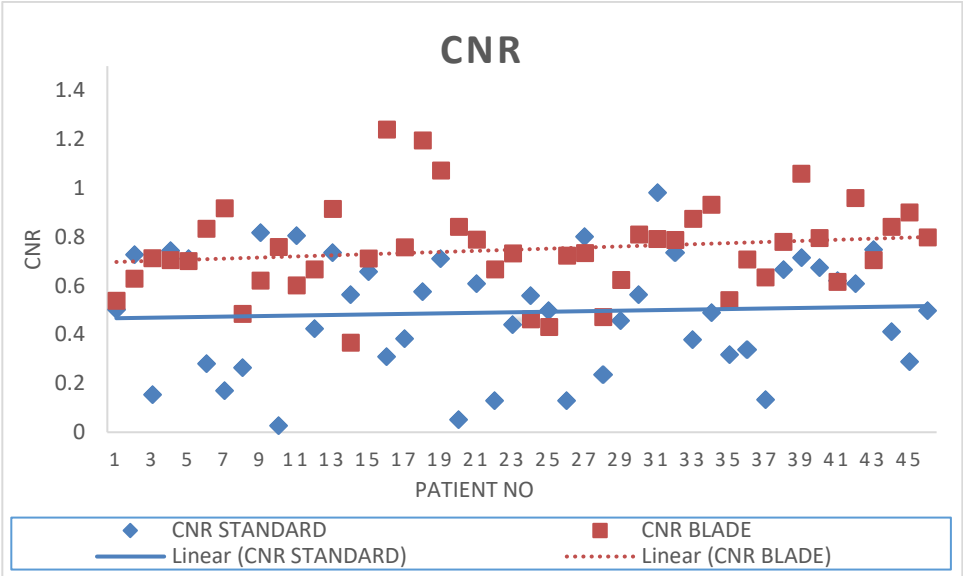


**Figure 7:** The contrast to noise ratio (CNR) between cerebrospinal fluid (CSF) and fat, the trend line of CNR of the BLADE sequence is higher than the CNR trend line of the standard sequence due to increased SNR and noise reduction.

The CNR is a vital part of our work, in order to determine the efficiency of fat and water suppression in our sequence. The higher the CNR, the more effective the suppression. Figure 4.5 shows the difference between the fat and water suppression around an optic nerve for both the BLADE and standard sequence.

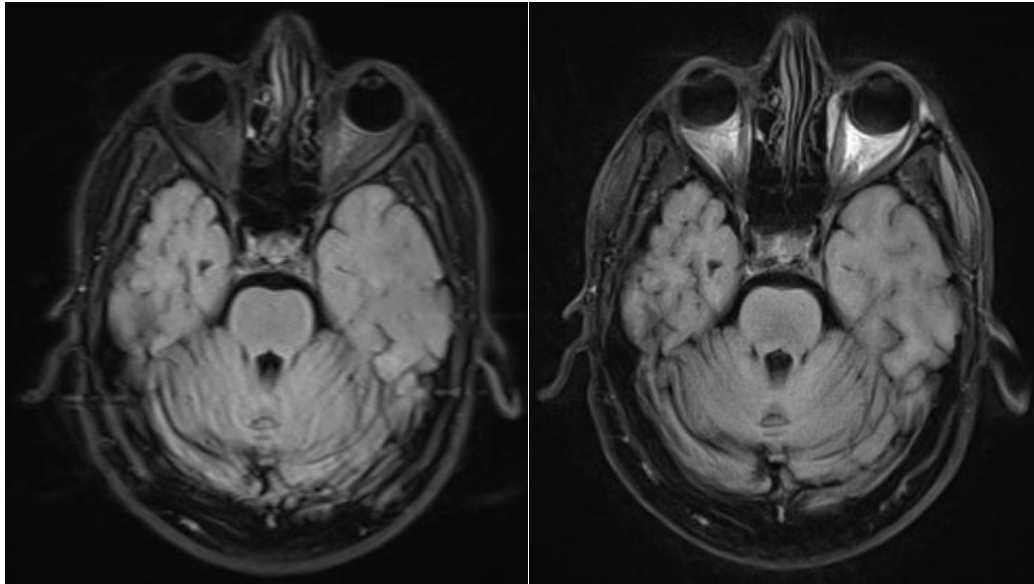


**Figure 8:** FLAIR Images with fat suppression, the left-hand side image exhibit cartesian filling for k-space, which shows successful fat suppression. While the right-hand side shows the BLADE sequence, which shows failed suppression sat around the optic nerve.

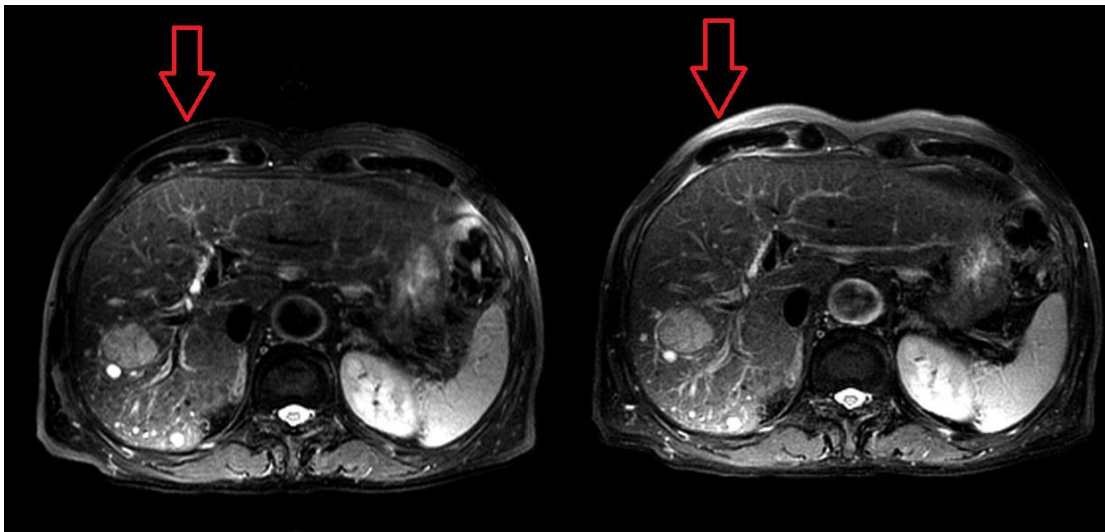


**Figure 9:** Axial liver MRI with fat suppression image adapted from a study by Sumire Nanko et al. in 2009, shows the same finding obtained in figure 7. Fat suppression is more efficient in the Cartesian image as shown in (the left-hand side image) (Sumire Nanko MD, Hidekazu Oshima MD, PhD, Takeshi Watanabe RT, Shigeru Sasaki MD, PhD, Masaki Hara MD, PhD, Yuta Shibamoto MD 2009).

The CNR equation (McRobbie et al. n.d.) shows that the SI in the numerator is increased due to the overlap in signal acquisition and inefficient fat suppression (Figure 6). This will lead to a higher overall SI. The increase in the SNR will result in a reduction in the background noise and an increase in the final CNR.

$$CNR_{\text{fat to CSF}} = SI_{\text{fat}} - SI_{\text{CSF}} / SD$$

### 4.3 Percentage of signal ghosting Values

The term ghosting refers to a type of structured noise that occurs when the signal instability between a pulse cycle's repetition occurs. It can be caused by either smearing, blurring, or shifting. Most commonly, ghosts appear along the phase encode direction. In the PSG test, the median value of all images was 0.50, and the measured values ranged from 0.0 to 1.91 (Figure 7). Although none of them failed, the values for the same image exhibited a dependence on the four rectangular ROIs. The presence of ghosts in standard images was due to the flow of cerebrospinal fluid (CSF) and eye movement. In these images, the ghost appeared in a few percentages and didn't affect the diagnosis value (Figure 8).

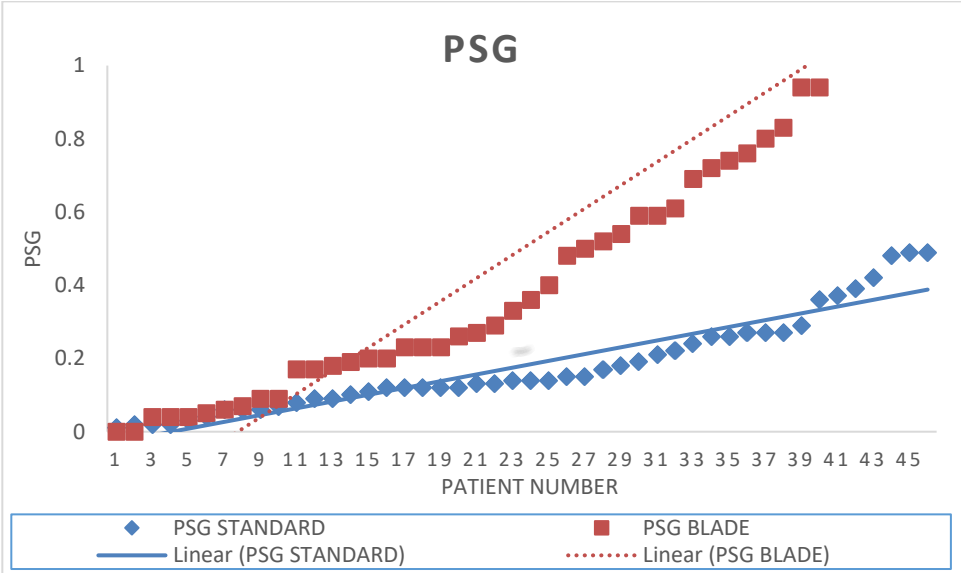


**Figure 10:** Percentage of signal ghosting (PSG) for BLADE and standard sequence. BLADE curve oscillates in the range between (0% and 1.91%) while the standard sequence PSG is less than 0.5% for all patients, the data exhibit ascending arrangement, and the PSG trend line of the BLADE sequence is higher than the PSG of the cartesian sequence both

trend line exhibit positive slope the PSG increase in BLADE sequence due to increase of motion in phase encoding direction.

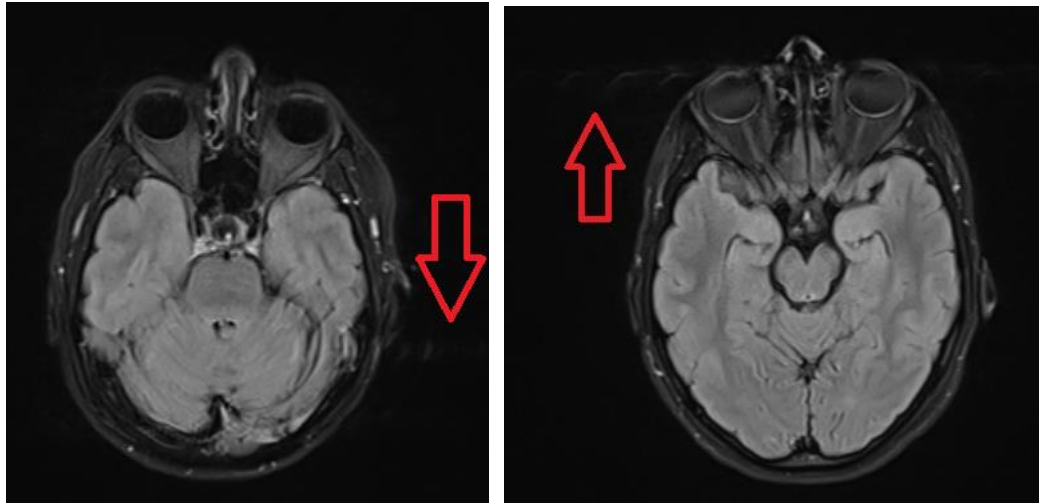


**Figure 10:** Left side image: arrow represent flow motion effect. Right side image: arrow represent eye movement effects on the image that appeared as a ghost artifact.

The cause of ghosting in the BLADE sequence was not due to the flow of blood nor eye movement, but rather to the patient's motion (mostly on the left side) as shown in (Figure 4.9). This was the main reason why the BLADE failed in its attempt to solve the issue of ghosting. As the phase encoding (PE) direction was right to left and theoretically ghosting appear in the PE direction (Mcrobbie et al. n.d.). The same results as Sedat Alibek et al. 2008, based on their finding, concluded that the pulsation artifacts are less common in the BLADE protocol. They also explained how this happens by applying the sequence to the central nervous system to eliminate motion and pulsation artifacts (Sedat Alibek 1 , Boris Adamietz, Alexander Cavallaro, Alto Stemmer, Katharina Anders, Manuel Kramer, Werner Bautz 2008).

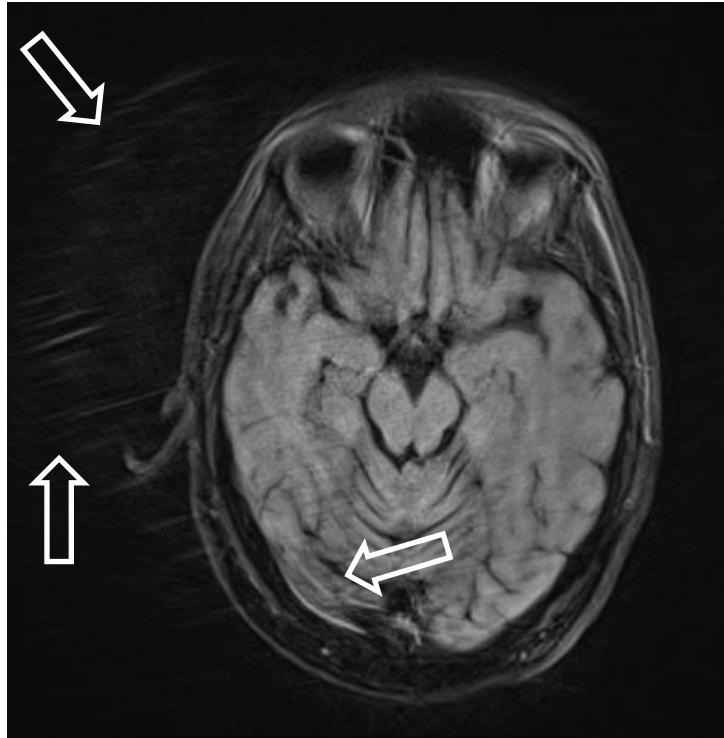


**Figure 11:** Ghost artifacts on the left side and inside of the image.

The dipole filling technique is useful in reducing the motion artifacts in the plane of in-plane motion (Figure 4.10). The central disc of this space is sampled by all BLADEs, and it is used as a 2D navigator. This allows for correction of the subject's internal rotation and translation, as well as identifying the BLADEs with corrupted data, and exclusion of these from the final reconstruction (Tamhane and Arfanakis 2009). However, it is not ideal in the cross-plane movement in the z-axis direction (Figure 4.11). When the patient head moves left or right rotation, the sequence may correct the motion artifact. However, the ghosting artifact shows up at the left side because of the phase encoding direction's right to left alignment. For patients with various motion, such as right bending, left bending, flexion and extension, the BLADE has less efficiency when it comes to solving the issue of motion artifact. This is because the data collected from other sections was used to reconstruct the slice (Tamhane and Arfanakis 2009).

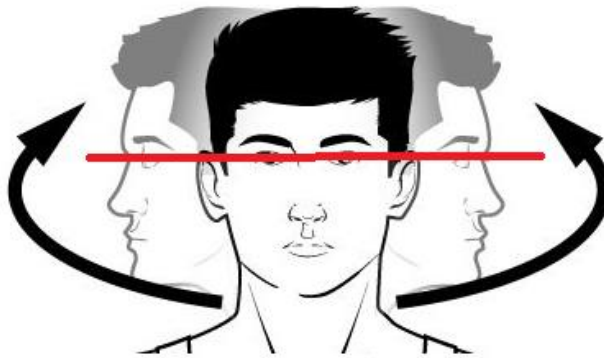


**Figure 12:** In-plan motion of the patient's head. The red line represents the slice section and patient motion in the range of the slice, so there was no data from outside the selected slice.

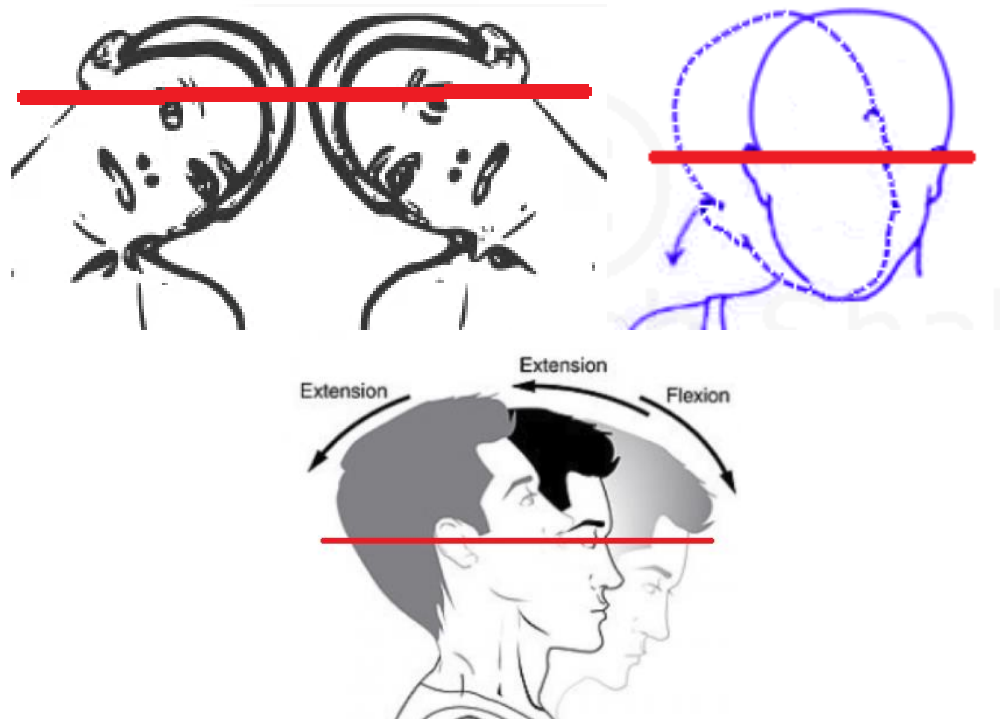


**Figure 13:** Cross-plan motion for the head. The slice section had changed and data were obtained from outside the slice.

Qualitative assessment hard to be done due to multiple factors, The image acceptance and rejection process is different between radiologists and radiographers. In addition, the skills of the observers and the legal responsibilities involved in rejecting or

accepting images are also different. It is concluded that the image quality and the image's appearance are dependent on the BLADE performance.

## **Chapter 5**

### **Conclusion and Recommendation**

#### **5.1. Conclusion**

Dipole filling for K-space can improve SNR, and CNR, and reduce ghosting in FLAIR images. The reduction of ghosting from CSF flow, eye movement, and slight motion can be achieved by using a dipole filling technique. However, the ghosting caused by severe motion was not able to be solved by the BLADE, also the ghosting in the phase encoding direction can't be solved by BLADE and worsening image quality with increasing the motion in the phase encoding direction as shown in figure 9 the PSG increased with increasing the motion in the phase encoding direction, also the fat sat technique efficiency in Cartesian filling more than dipole filling, the strong fat sat in Cartesian filling, appeared some time weak and some time without fat sat as shown in figure 7.

#### **5.2. Recommendation**

The FLAIR sequence can be used to enhance the CNR and SNR, and reduce CSF flow artifact, eye motion artifact and manage the motion of patients and reduce the need for anesthesia, this sequence can be used for uncooperative patients, Pediatric patients, and patients with involuntary motion.



## References

- Alibek, Sedat, Boris Adamietz, Alexander Cavallaro, Alto Stemmer, Katharina Anders, Manuel Kramer, Werner Bautz, and Gundula Staatz. 2008. "Contrast-Enhanced T1-Weighted Fluid-Attenuated Inversion-Recovery BLADE Magnetic Resonance Imaging of the Brain." *Academic Radiology* 15(8):986–95. doi: 10.1016/j.acra.2008.03.009.
- Almuqbel, Mustafa M., Gareth Leeper, David N. Palmer, Nadia L. Mitchell, Katharina N. Russell, Ross J. Keenan, and Tracy R. Melzer. 2018. "Practical Implications of Motion Correction with Motion Insensitive Radial k -Space Acquisitions in MRI." *The British Journal of Radiology* 20170593. doi: 10.1259/bjr.20170593.
- Andre, Jalal B., Brian W. Bresnahan, Mahmud Mossa-Basha, Michael N. Hoff, C. Patrick Smith, Yoshimi Anzai, and Wendy A. Cohen. 2015. "Toward Quantifying the Prevalence, Severity, and Cost Associated with Patient Motion during Clinical MR Examinations." *Journal of the American College of Radiology* 12(7):689–95. doi: 10.1016/j.jacr.2015.03.007.
- Barton F. Lane<sup>1</sup>, Fauzia Q. Vandermeer<sup>1</sup>, Rasim C. Oz<sup>1 2</sup>, Eric W. Irwin<sup>1 3</sup>, Alan B. McMillan<sup>1</sup> and Jade J. Wong-You-Cheong<sup>1</sup>. 2011. "Comparison of Sagittal T2-Weighted BLADE and Fast Spin-Echo MRI of the Female Pelvis for Motion Artifact and Lesion Detection." *AJR* 197.
- Boussel, Loic, Gwenael Herigault, Alejandro De La Vega, Michel Nonent, Philippe Charles Douek, and Jean Michel Serfaty. 2006. "Swallowing, Arterial Pulsation, and Breathing Induce Motion Artifacts in Carotid Artery MRI." *Journal of Magnetic Resonance Imaging* 23(3):413–15. doi: 10.1002/jmri.20525.
- van Dijk, Koene R. A., Mert R. Sabuncu, and Randy L. Buckner. 2012. "The Influence of

- Head Motion on Intrinsic Functional Connectivity MRI.” *NeuroImage* 59(1):431–38.  
doi: 10.1016/j.neuroimage.2011.07.044.
- Epistatou, Angeliki C., Ioannis A. Tsalafoutas, and Konstantinos K. Delibasis. 2020. “An Automated Method for Quality Control in MRI Systems: Methods and Considerations.” *Journal of Imaging* 6(10). doi: 10.3390/jimaging6100111.
- Henrik J. Michaely MD, Harald Kramer MD, Sabine Weckbach MD, Olaf Dietrich PhD, Maximilian F. Reiser MD, Stefan O. Schoenberg PhD. 2008. “Renal T2-Weighted Turbo-Spin-Echo Imaging with BLADE at 3.0 Tesla: Initial Experience.” *JMRI* 27(1):148–53.
- Huyen Thanh Nguyen 1 , Zarine Ketul Shah 1 , Amir Mortazavi 2 , Kamal S Pohar 3 , Lai Wei 4 , Debra Lyn Zynger 5, Michael Vinzenz Knopp 1. n.d. “Periodically Rotated Overlapping Parallel Lines with Enhanced Reconstruction Acquisition to Improve Motion-Induced Artifacts in Bladder Cancer Imaging: Initial Findings.” *Medicine* 98.
- Lavdas, Eleftherios, Panayiotis Mavroidis, Spiros Kostopoulos, Dimitrios Glotsos, Violeta Roka, Theofilos Topalzikis, Athanasios Bakas, Georgia Oikonomou, Nikos Papanikolaou, Georgios Batsikas, Ioannis Kaffes, and Dimitrios Kechagias. 2013. “Improvement of Image Quality Using BLADE Sequences in Brain MR Imaging.” *Magnetic Resonance Imaging* 31(2):189–200. doi: 10.1016/j.mri.2012.08.001.
- Lin Zhang, ChunMei Tian, PeiYuan Wang, Liang Chen, XiJin Mao, ShanShan Wang, Xu Wang, JingMin Dong & Bin Wang. 2015. “Comparative Study of Image Quality between Axial T2-Weighted BLADE and Turbo Spin-Echo MRI of the Upper Abdomen on 3.0 T.” *Japanese Journal of Radiology* 33:585–90.
- Mcrobbie, Donald W., Elizabeth A. Moore, Martin J. Graves, and Martin R. Prince. n.d. *MRI from Picture to Proton MRI from Picture to Proton.*

- Ohgiya, Yoshimitsu, Jumpei Suyama, Noritaka Seino, Shu Takaya, Masaaki Kawahara, Makoto Saiki, Syouei Sai, Masanori Hirose, and Takehiko Gokan. 2010. "MRI of the Neck at 3 Tesla Using the Periodically Rotated Overlapping Parallel Lines with Enhanced Reconstruction (PROPELLER) (BLADE) Sequence Compared with T2-Weighted Fast Spin-Echo Sequence." *Journal of Magnetic Resonance Imaging* 32(5):1061–67. doi: 10.1002/jmri.22234.
- Pipe, James G. 1999. "Motion Correction with PROPELLER MRI: Application to Head Motion and Free-Breathing Cardiac Imaging." *Magnetic Resonance in Medicine* 42(5):963–69. doi: 10.1002/(SICI)1522-2594(199911)42:5<963::AID-MRM17>3.0.CO;2-L.
- R. George, J. , Dela Cruz, R. singh. 2022. "Signal to Noise Ratio (SNR) and Image Quality." Retrieved (<https://mrimaster.com/technique SNR.html>).
- Satterthwaite, Theodore D., Daniel H. Wolf, James Loughead, Kosha Ruparel, Mark A. Elliott, Hakon Hakonarson, Ruben C. Gur, and Raquel E. Gur. 2012. "Impact of In-Scanner Head Motion on Multiple Measures of Functional Connectivity: Relevance for Studies of Neurodevelopment in Youth." *NeuroImage* 60(1):623–32. doi: 10.1016/j.neuroimage.2011.12.063.
- Sedat Alibek 1 , Boris Adamietz, Alexander Cavallaro, Alto Stemmer, Katharina Anders, Manuel Kramer, Werner Bautz, Gundula Staatz. 2008. "Contrast-Enhanced T1-Weighted Fluid-Attenuated Inversion-Recovery BLADE Magnetic Resonance Imaging of the Brain: An Alternative to Spin-Echo Technique for Detection of Brain Lesions in the Unsedated Pediatric Patient?" *NIH* 8:986–95.
- Shokrollahi, Peyman, James M. Drake, and Andrew A. Goldenberg. 2017. "Signal-to-Noise Ratio Evaluation of Magnetic Resonance Images in the Presence of an Ultrasonic

Motor.” *BioMedical Engineering Online* 16(1):1–12. doi: 10.1186/s12938-017-0331-1.

Siegelman ES, Outwater EK. n.d. “Tissue Characterization in the Female Pelvis Utilizing MR Imaging.” *Radiology* 212:5–18.

Sumire Nanko MD, Hidekazu Oshima MD, PhD, Takeshi Watanabe RT, Shigeru Sasaki MD, PhD, Masaki Hara MD, PhD, Yuta Shibamoto MD, PhD. 2009. “Usefulness of the Application of the BLADE Technique to Reduce Motion Artifacts on Navigation-Triggered Prospective Acquisition Correction (PACE) T2-Weighted MRI (T2WI) of the Liver.” *JMRI* 30(2):321–26.

Tamhane, Ashish A., and Konstantinos Arfanakis. 2009. “Motion Correction in Periodically-Rotated Overlapping Parallel Lines with Enhanced Reconstruction (PROPELLER) and Turboprop MRI.” *Magnetic Resonance in Medicine* 62(1):174–82. doi: 10.1002/mrm.22004.

Wu, Lin, Shuang Zhang, and Tao Zhang. 2021. “Mri-Based Image Signal-to-Noise Ratio Enhancement with Different Receiving Gains in k-Space.” *Sensors* 21(16):1–15. doi: 10.3390/s21165296.

Yuusuke Hirokawa MD, Hiroyoshi Isoda PhD, Yoji S. Maetani PhD, Shigeki Arizono MD, Kotaro Shimada MD, Kaori Togashi PhD. 2008. “Evaluation of Motion Correction Effect and Image Quality with the Periodically Rotated Overlapping Parallel Lines with Enhanced Reconstruction (PROPELLER) (BLADE) and Parallel Imaging Acquisition Technique in the Upper Abdomen.” 28(4).

# فعالية الملء القطبي في حل مشكلة الحركة لبروتوكول تثبيط السوائل في صور الرنين

## المغناطيسي الخاصة بالدماغ

اعداد الطالبة: مرام محمد مطيع غزاونة

اشراف: د. محمد حجوج

### الملخص

التصوير بالرنين المغناطيسي (MRI) يوفر معلومات مفصلة حول التشريح الداخلي لجسم المريض, ويعد استخدام بروتوكول تثبيط اشارة السوائل (FLAIR) ذو أهمية في تصوير الدماغ حيث يساعد على التمييز بين السوائل وامراض الدماغ, ومع الأسف ليس من الممكن الحصول على صورة تشخيصية في جميع الحالات نظرا لحساسية التصوير بالرنين المغناطيسي لحركة المريض هذه الحركة تؤثر على القيمة التشخيصية للصورة, في هذه الدراسة نسعى لدراسة أثر الملء القطبي للبيانات ل 46 صورة تم تصويرها ب حركات مختلفة بحيث تشمل هذه الحركات دوران لليمين, دوران للييسار, انحناء لليمين, انحناء للييسار, انحناء للأمام, وانحناء للخلف. قمنا في هذه الدراسة بحساب نسبة التباين, نسبة الإشارة الى التشويش, ونسبة الإشارة الوهمية. حيث تم استخدام برنامج RADIANT DICOM لقياس كثافة الإشارة والانحراف المعياري للإشارة, ويستخدم الانحراف المعياري كمؤشر على كمية التشويش. استخدمنا أيضا في هذه الدراسة برنامج imageQC لحساب نسبة الإشارة الوهمية. تم تسجيل النتائج على برنامج مايكروسوفت اكسل وتمت مقارنتها ب 46 صورة تم اجرائها بالبروتوكول المعياري الذي يستخدم الملء الخطي للبيانات, أظهرت النتائج تحسنا في نسبة الإشارة الى التشويش ونسبة التباين, بالإضافة الى حل مشكلة الإشارة الوهمية الناتجة عن تدفق السائل النخاعي وحركة رموش العين بينما لم يتم تصحيح الإشارة الوهمية الناتجة عن الحركات المتكررة للمريض, كان متوسط نسبة الإشارة الى التشويش في الصور التي تم اجرائها باستخدام الملء القطبي 1.08 بينما صور الملء الخطي 0.92 حيث يعتبر فرق ذو دلالة إحصائية عند قيمة احتمالية اقل من 5%, وبالنسبة لنسبة التباين لصور الملء القطبي 0.75 وانخفض الى 0.49 في صور الملء الخطي ويعتبر هذا فرق ذو دلالة إحصائية عند قيمة احتمالية اقل من 5%. ختاماً نسبة الإشارة الوهمية 0.75 في صور الملء القطبي وانخفض الى 0.18 في صور الملء الخطي حيث يعتبر هذا فرق ذو دلالة إحصائية عند قيمة احتمالية اقل من 5%. ونستنتج ان الملء القطبي يعزز نسبة التباين ونسبة الإشارة الى التشويش ويحل مشكلة الإشارة الوهمية الناتجة عن تدفق السائل النخاعي وحركة العين بينما يفشل في حل مشكلة الحركات المتكررة.